

Finite-Field Ground State of the $S = 1$ Antiferromagnetic-Ferromagnetic Bond-Alternating Chain

Takashi Tonegawa¹, Kiyomio Kamoto² and Makoto Kaburagi³

¹Department of Mechanical Engineering, Fukui University of Technology, Fukui 910-8505, Japan

²Department of Physics, Tokyo Institute of Technology, Tokyo 152-8551, Japan

³Faculty of Cross-Cultural Studies, Kobe University, Kobe 657-8501, Japan

We investigate the finite-field ground state of the $S = 1$ antiferromagnetic-ferromagnetic bond-alternating chain described by the Hamiltonian $H = \sum_i S_{2i-1} \cdot S_{2i} + JS_{2i} \cdot S_{2i+1} + D \sum_i (S_i^z)^2$, where $J > 0$ and $0 < D < 1$. We find that two kinds of magnetization plateaux at a half of the saturation magnetization, the $\frac{1}{2}$ -plateaux, appear in the ground-state magnetization curve; one of them is of the Haldane type and the other is of the large- D type. We determine the $\frac{1}{2}$ -plateau phase diagram on the D versus J plane, applying the twisted-boundary-condition level spectroscopy methods developed by Kitazawa and Nomura. We also calculate the ground-state magnetization curves and the magnetization phase diagrams by means of the density-matrix renormalization-group method.

KEYWORDS: $S = 1$ antiferromagnetic-ferromagnetic bond-alternating chain, numerical methods, ground-state magnetization curve, $\frac{1}{2}$ -plateau phase diagram, magnetization phase diagram

1. Introduction

There has been a considerable current interest in the study of the ground-state properties of various one-dimensional quantum spin systems in a finite magnetic field. In this paper we discuss the case of the $S = 1$ bond-alternating chain, for which we express the Hamiltonian in the following form:

$$H = H_{\text{ex}} + H_Z; \quad (1)$$

$$H_{\text{ex}} = \sum_i S_{2i-1} \cdot S_{2i} + JS_{2i} \cdot S_{2i+1} + D \sum_i (S_i^z)^2; \quad (2)$$

$$H_Z = H \sum_i S_i^z; \quad (3)$$

where S_i is the $S = 1$ operator at the i th site; J ($0 < J < 1$) is the parameter representing the bond alternation of the nearest-neighbor interactions; D ($0 < D < 1$) is the uniaxial single-ion-type anisotropy constant; H ($H > 0$) is the magnitude of the external magnetic field applied along the z -direction. Hereafter, we denote by M the z component of the total spin $S_{\text{tot}} = \sum_{i=1}^N S_i^z$, where N , being assumed to be a multiple of four, is the total number of spins in the system.

The finite-field as well as the zero-field ground-state properties of the present system in the case of the antiferromagnetic-antiferromagnetic bond-alternating chain with $J > 0$ have already been investigated by using mainly numerical methods.^{1,2} As for the zero-field properties, the ground-state phase diagram on the J versus D plane, in which the Neel, Haldane, large- D , and dimer phases appear, has been determined.^{1,2} On the other hand, the results for the ground-state magnetization curve show that the magnetization plateau at a half of the saturation magnetization, which is called the $\frac{1}{2}$ -plateau, appears for arbitrary values of J except for $J = 1$ at least when $D = 0$.¹

In this study we explore the finite-field ground-state properties of the system in the case of the antiferromagnetic-ferromagnetic bond-alternating chain with $J < 0$, focusing our attention mainly upon the $\frac{1}{2}$ -plateau appearing in the magnetization curve. When $D = 0$, the present system is mapped onto the isotropic $S = 2$ uniform antiferromagnetic chain in the limit of $J \rightarrow 1$. Thus, it is considered that, no plateau appears in the ground-state magnetization curve in this limit when $D = 0$. As we have already discussed,¹ on the other hand, the $\frac{1}{2}$ -plateau appears when $J = 0$ and $D > \frac{2}{3}$. These imply that the ' $\frac{1}{2}$ -plateau'-no-plateau' transition occurs at a finite value of J for a certain region of D including $D = 0$. Furthermore, as has already been shown,³ the magnetization plateau at one third of the saturation magnetization, the $\frac{1}{3}$ -plateau, appearing in the ground-state magnetization curve of the $S = \frac{3}{2}$ uniform antiferromagnetic chain with single-ion-type anisotropy changes its character from the Haldane-type to the large- D type at a finite value of the anisotropy constant. We expect that this type of Haldane-type- $\frac{1}{2}$ -plateau'-large- D type- $\frac{1}{2}$ -plateau' transition may take place also in the present $S = 1$ antiferromagnetic-ferromagnetic bond-alternating chain. To discuss quantitatively these transitions and to complete the $\frac{1}{2}$ -plateau phase diagram on the D versus J plane are our main purposes. We also aim at calculating the magnetization phase diagram as well as the ground-state magnetization curve.

In the next section (x2) we discuss the $\frac{1}{2}$ -plateau phase diagram. In determining the phase diagram, we apply the twisted-boundary-condition level spectroscopy (TBCLS) analyses of the numerical diagonalization data, developed by Kitazawa⁴ and also by Nomura and Kitazawa.⁵ Then, we discuss in x3 the ground-state magnetization curve, which we calculate by using the density-matrix renormalization-group (DMRG) method proposed originally by White.⁶ We also discuss the magnetization phase

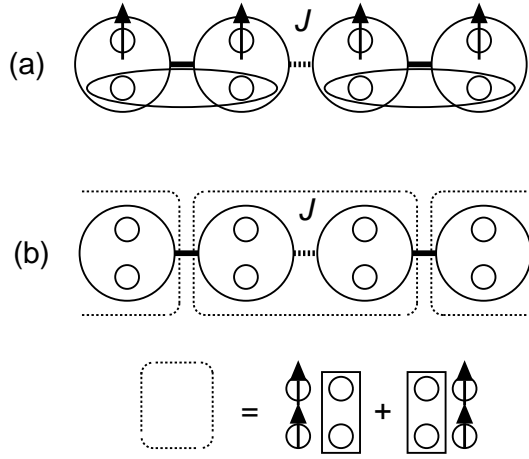


Fig. 1. Schematic pictures representing (a) the Haldane-type- $\frac{1}{2}$ -plateau' phase and (b) the 'large-D-type- $\frac{1}{2}$ -plateau' phase. The thick solid and dotted lines stand, respectively, for the antiferromagnetic and ferromagnetic bonds, and the small open circles for the $S = \frac{1}{2}$ spins. Each large open circle surrounding two $S = \frac{1}{2}$ spins stands for an operation of constructing an $S = 1$ spin by symmetrization. The $S = \frac{1}{2}$ spin with an upward arrow is in the up state ". Furthermore, two $S = \frac{1}{2}$ spins in a ellipse form a singlet dimer $\frac{1}{2} \uparrow \downarrow \downarrow \uparrow$, and two $S = \frac{1}{2}$ spins in a rectangular form a triplet dimer $\frac{1}{2} \uparrow \uparrow \downarrow \downarrow$.

diagram which is obtained from the result for the magnetization curve. Finally, concluding remarks are given in §4.

2. $\frac{1}{2}$ -Plateau Phase Diagram

From the considerations presented in the previous section, it is expected that three phases, i.e., the 'ho-plateau', Haldane-type- $\frac{1}{2}$ -plateau', and 'large-D-type- $\frac{1}{2}$ -plateau' phases appear in the $\frac{1}{2}$ -plateau phase diagram. Schematic pictures in terms of a kind of the valence-bond-solid picture, which represents the latter two phases, are shown in Fig. 1.

We can determine the transition lines between two of the above three phases rather precisely by applying the TBCLS methods in the following way. Both the Haldane-type- $\frac{1}{2}$ -plateau'-ho-plateau' transition and the 'large-D-type- $\frac{1}{2}$ -plateau'-ho-plateau' transition are the Berezinskii-Kosterlitz-Thouless transition⁷ accompanying no spontaneous breaking of the translational symmetry of the Hamiltonian H . Therefore, the critical points $J_c^{(H;mo)}$ and $J_c^{(L;D;mo)}$ of J , which are, respectively, for the former and latter transitions, for a given value of D (or, $D_c^{(H;mo)}$ and $D_c^{(L;D;mo)}$ of D for a given value of J) can be estimated by means of Nomura and Kitazawa's TBCLS method.⁵ We denote by $E_0^{(P)}(N;M)$ the lowest energy eigenvalue of H_{ex} with the periodic boundary condition within the subspace determined by the values of N and M , and also by $E_0^{(T)}(N;M;P)$ the lowest energy eigenvalue of H_{ex} with the twisted boundary condition within the subspace determined by the values of N , M , and P , where P is the eigenvalue of the space inversion operator. Then, Nomura and Kitazawa's TBCLS method⁵ predicts that $J_c^{(H;mo)}(D_c^{(H;mo)})$ is obtained by extrapolating

$J_c^{(H;mo)}(N)$, $D_c^{(H;mo)}(N)$ determined from the equation

$$E_0^{(T)}(N; \frac{N}{2}; 1) = \frac{1}{2} E_0^{(P)}(N; \frac{N}{2} + 2) + E_0^{(P)}(N; \frac{N}{2} - 2) \quad (4)$$

to $N \rightarrow 1$. Similarly, $J_c^{(L;D;mo)}(D_c^{(L;D;mo)})$ is obtained by extrapolating $J_c^{(L;D;mo)}(N)$, $D_c^{(L;D;mo)}(N)$ determined from

$$E_0^{(T)}(N; \frac{N}{2}; +1) = \frac{1}{2} E_0^{(P)}(N; \frac{N}{2} + 2) + E_0^{(P)}(N; \frac{N}{2} - 2) \quad (5)$$

to $N \rightarrow 1$.

On the other hand, the Haldane-type- $\frac{1}{2}$ -plateau'-'large-D-type- $\frac{1}{2}$ -plateau' transition is expected to be of the Gaussian type as in the case of the Haldane-type- $\frac{1}{3}$ -plateau'-'large-D-type- $\frac{1}{3}$ -plateau' transition in the $S = \frac{3}{2}$ uniform antiferromagnetic chain with single-ion-type anisotropy,³ discussed in the previous section. Thus, we can apply Kitazawa's TBCLS method⁴ to estimate the critical point $J_c^{(H;LD)}$ of J for a given D (or, $D_c^{(H;LD)}$ for a given J) in this transition. According to this method, $J_c^{(H;LD)}(D_c^{(H;LD)})$ can be estimated by extrapolating $J_c^{(H;LD)}(N)$, $D_c^{(H;LD)}(N)$ determined from

$$E_0^{(T)}(N; \frac{N}{2}; +1) = E_0^{(T)}(N; \frac{N}{2}; 1) \quad (6)$$

to $N \rightarrow 1$. It is noted that in the limit of $N \rightarrow 1$, the value of $E_0^{(T)}(N; \frac{N}{2}; 1)$ is smaller or larger than that of $E_0^{(T)}(N; \frac{N}{2}; +1)$ depending upon whether in the Haldane-type- $\frac{1}{2}$ -plateau' region or in the 'large-D-type- $\frac{1}{2}$ -plateau' region.

Determining the $\frac{1}{2}$ -plateau phase diagram on the D versus J plane, we have first calculated numerically the energy eigenvalues $E_0^{(P)}(N; \frac{N}{2} + 2)$, $E_0^{(P)}(N; \frac{N}{2} - 2)$, $E_0^{(T)}(N; \frac{N}{2}; +1)$, and $E_0^{(T)}(N; \frac{N}{2}; 1)$ for a variety of values of J and D for finite-size systems with $N = 8, 12$, and 16 spins, employing the computer program package KOBEPACK⁸ coded by means of the Lanczos technique. Then, we have solved numerically eqs. (4), (5), and (6), respectively, to evaluate $J_c^{(H;mo)}(N)$, $D_c^{(H;mo)}(N)$, $J_c^{(L;D;mo)}(N)$, $D_c^{(L;D;mo)}(N)$, and $J_c^{(H;LD)}(N)$, $D_c^{(H;LD)}(N)$. Finally, we have extrapolated these finite-size values to $N \rightarrow 1$ to estimate $J_c^{(H;mo)}(D_c^{(H;mo)})$, $J_c^{(L;D;mo)}(D_c^{(L;D;mo)})$, and $J_c^{(H;LD)}(D_c^{(H;LD)})$ by assuming that the N -dependences of the finite-size values are quadratic functions of N^{-2} . Plotting the extrapolated results on the D versus J plane, we have obtained the $\frac{1}{2}$ -plateau phase diagram as depicted in Fig. 2. It is noted that, for example, $J_c^{(H;mo)} = 1.69 \pm 0.01$ for $D = 0$. Furthermore, the three transition lines in the phase diagram meet at the point ($J = 8.13 \pm 0.01, D = 1.19 \pm 0.01$).

As can be seen from Fig. 2, the 'large-D-type- $\frac{1}{2}$ -plateau'-ho-plateau' transition line is almost parallel to

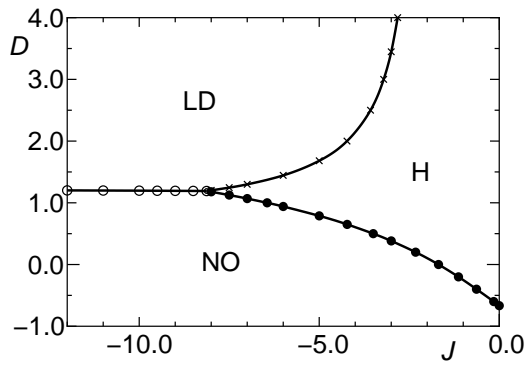


Fig. 2. $\frac{1}{2}$ -plateau phase diagram on the D versus J plane. Here, NO, H, and LD stand, respectively, for the 'no-plateau', 'Haldane-type $\frac{1}{2}$ -plateau', and 'large-D-type $\frac{1}{2}$ -plateau' regions. The three transition lines meet at the point ($J = -8.13 \pm 0.01$, $D = 1.19 \pm 0.01$), which is marked by the double circle.

the J -axis in the whole region of $J < -8.13$. This result may be attributed to the fact that the present $S = 1$ system in this region is almost equivalent to the $S = 2$ uniform antiferromagnetic chain with single-ion-type anisotropy, since $|J|$ is fairly large with $J < 0$. Thus, we may expect a direct transition from the 'no-plateau' phase to the 'large-D-type $\frac{1}{2}$ -plateau' one in the above $S = 2$ chain, in contrast to the case of the $\frac{1}{3}$ -plateau in the corresponding $S = \frac{3}{2}$ chain,³ mentioned in x1. Figure 2 also shows that the 'large-D-type $\frac{1}{2}$ -plateau' phase appears when both $|J|$ ($J < 0$) and D ($D > 0$) are sufficiently large. The fitting of several values of $J_c^{(H;LD)}$ for sufficiently large D 's to a quadratic function of D^{-1} suggests that the 'Haldane-type $\frac{1}{2}$ -plateau'-'large-D-type $\frac{1}{2}$ -plateau' transition line approaches $J = -2.05 \pm 0.05$ in the limit of $D \rightarrow 1$.

3. Magnetization Curve and Magnetization Phase Diagram

Let us begin with discussing the saturation field H_s for the present system in the case of $J < 0$. It is given by

$$H_s = E_0^{(F)}(N; N) - E_0^{(F)}(N; N-1) = D + 2 \quad (7)$$

or

$$H_s = \frac{1}{2} \lim_{N \rightarrow \infty} \frac{E_0^{(F)}(N; N) - E_0^{(F)}(N; N-2)}{N} = \frac{1}{2} E_B \quad (8)$$

depending on whether $2(D+2) > E_B$ or $2(D+2) < E_B$, where E_B is the maximum energy of the ferromagnetic two-magnon bound state. In principle, the energy E_B can be calculated analytically. However, this calculation in the case of $J \neq 1$ has not yet been done as far as we know,¹⁰ and therefore we estimate H_s numerically when $2(D+2) < E_B$.

We have applied the DMRG method⁶ to calculate the ground-state magnetization curve, which we define here as the average magnetization $m(N)$ ($M = N$) per spin versus the reduced field $H = H_s$ curve. In this application, we usually have to impose open boundary conditions for the Hamiltonian treated. In the present system, we have two kinds of open boundary conditions, Oa and Of,

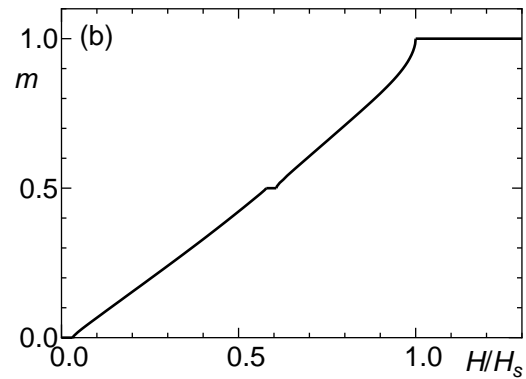
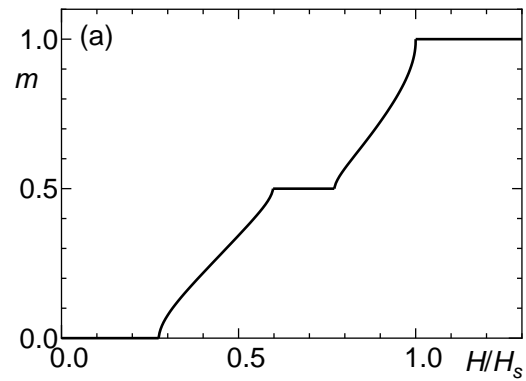


Fig. 3. Ground-state magnetization curves in the $N \rightarrow \infty$ limit obtained for the cases of (a) $J = -1.0$ and $D = 3.0$ and of (b) $J = -10.0$ and $D = 3.0$

which are, respectively, the cases where the edge bonds are the antiferromagnetic and ferromagnetic bonds. We adopt, respectively, the Oa and Of conditions when we calculate the magnetization curves in the 'Haldane-type $\frac{1}{2}$ -plateau' and 'large-D-type $\frac{1}{2}$ -plateau' regions. This is because, as can be seen from the schematic pictures for these phases shown in Fig. 1, no degrees of freedom appear at both edges of the chain in the above adoption, which leads to a less boundary effect.

We have calculated the lowest energy eigenvalue $E_0^{(Ox)}(N; M)$ ($x = f$ or a) under the open boundary condition Ox of H_{ex} within the subspace determined by the values of N and M for $N = 36, 64$, and 84 and for all values of M ($M = 0, 1, \dots, N$). From these results the ground-state magnetization curves for $N = 36, 64$, and 84 can be readily obtained.⁹ The resulting magnetization curve for each N is a stepwise increasing function of H , starting from $m(N) = 0$ at $H = H_0(N)$ and reaching to the saturation value $m(N) = 1$ at $H = H_s(N)$. We note that $H_s = \lim_{N \rightarrow \infty} H_s(N)$.

Except for plateau regions, a satisfactorily good approximation to the magnetization curve in the $N \rightarrow \infty$ limit, i.e., the $m(l)$ versus $H = H_s$ curve, may be obtained by drawing a smooth curve through the midpoints of the steps in the finite-size magnetization curves.⁹ As for the estimations of $H_0 = H_0(l)$, which is nothing but the energy gap between the ground state and a first excited state in the case of $H = 0$, as well as of H_1 and H_2 , which are the lowest and highest val-

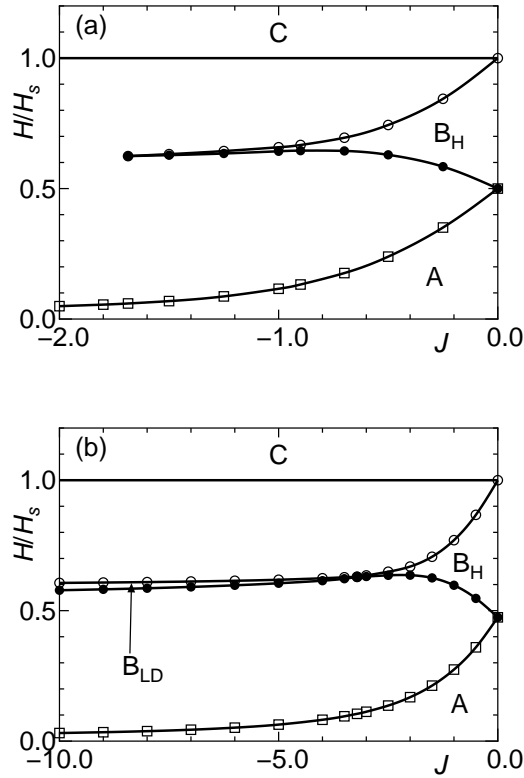


Fig. 4. Magnetization phase diagrams on the $H=H_s$ versus J plane obtained for the cases of (a) $D = 0.0$ and (b) $D = 3.0$, where $H_0=H$ (open squares), $H_1=H$ (solid circles), and $H_2=H$ (open circles) are plotted as functions of J . In the regions A, B_X ($X=H$ or LD), and C, the average magnetization m per spin is equal to 0 (the 0-plateau region), $\frac{1}{2}$ (the $\frac{1}{2}$ -plateau region), and 1 (the saturated magnetization region); the B_H and B_{LD} regions are, respectively, the 'Haldane-type $\frac{1}{2}$ -plateau' and 'large-D-type $\frac{1}{2}$ -plateau' regions. In other regions, m increases continuously with the increase of $H=H_s$.

ues of H giving the $\frac{1}{2}$ -plateau, respectively, we extrapolate the corresponding results for $N = 36, 64$, and 84 to $N \rightarrow \infty$, assuming again the N -dependences of the finite-size values are quadratic functions of N^{-2} . The magnetization curve thus obtained for the cases of $J = -1.0$ and $D = 3.0$ and of $J = -10.0$ and $D = 3.0$, which are, respectively, in the 'Haldane-type $\frac{1}{2}$ -plateau' and 'large-D-type $\frac{1}{2}$ -plateau' regions (see Fig. 2), are depicted in Fig. 3.

The magnetization phase diagram on the $H=H_s$ versus J plane for a given value of D is obtained by plotting H_0, H_1, H_2 , and H_s as a function of J . The results for the cases of $D = 0.0$ and $D = 3.0$ are shown in Fig. 4. Figure 4(a) demonstrates that in the case of $D = 0.0$, the $\frac{1}{2}$ -plateau, which is of the 'Haldane-type', appears when $-1.69 < J < 0.0$, and Fig. 4(b) shows that in the case of $D = 3.0$, the $\frac{1}{2}$ -plateau disappears at the critical point $J_c^{(H, LD)} = -3.21$ for the 'Haldane-type $\frac{1}{2}$ -plateau'-'large-D-type $\frac{1}{2}$ -plateau' phase transition (see Fig. 2).

4. Concluding Remarks

We have investigated the infinite-dimensional ground state of the $S = 1$ antiferromagnetic-ferromagnetic bond-alternating

chain described by the Hamiltonian H [see eqs. (1-3)] with $J > 0$ and $1 < D < \infty$, focusing our attention mainly upon the $\frac{1}{2}$ -plateau appearing in the magnetization curve. We have found that two kinds of magnetization plateaux, i.e., the 'Haldane-type $\frac{1}{2}$ -plateau' and the 'large-D-type $\frac{1}{2}$ -plateau' [Fig. 1] appear. We have determined the $\frac{1}{2}$ -plateau phase diagram on the D versus J plane [Fig. 2], applying the TBCLS methods.^{4,5} We have also calculated, by means of the DMRG method,⁶ the ground-state magnetization curves for a variety of values of J with D fixed at $D = 0.0$ and 3.0 , two examples of which being presented [Fig. 3]. Using the results for the magnetization curves, we finally obtained the magnetization phase diagrams on the $H=H_s$ versus J plane for $D = 0.0$ and 3.0 [Fig. 4].

For the purpose of exploring the effect of frustration, we are now studying the case where the antiferromagnetic next-nearest-neighbor interaction term J_2 ($S_i \cdot S_{i+2}$, $J_2 > 0$) is added to the Hamiltonian of eqs. (1-3), assuming either $J > 0$ or $J < 0$. It is noted that when $J = 0$, the system is reduced to the $S = 1$ antiferromagnetic ladder, where the ratio of the leg interaction constant to the rung one is J_2 . The results will be published in the near future.

Acknowledgments

We wish to thank Professor T. Hikihara by whom the DMRG program used in this study is coded. We also thank the Supercomputer Center, Institute for Solid State Physics, University of Tokyo, the Information Synergy Center, Tohoku University, and the Computer Room, Yukawa Institute for Theoretical Physics, Kyoto University for computational facilities. The present work has been supported in part by Grants-in-Aid for Scientific Research (C) (No. 16540332, No. 14540329, and No. 14540358) and a Grant-in-Aid for Scientific Research on Priority Areas (B) (Field-Induced New Quantum Phenomena in Magnetic Systems) from the Ministry of Education, Culture, Sports, Science and Technology.

- 1) T. Tonegawa, T. Nakao and M. Kaburagi: J. Phys. Soc. Jpn. 65 (1996) 3317.
- 2) W. Chen, H. Hida and B. C. Sanctuary: J. Phys. Soc. Jpn. 69 (2000) 237.
- 3) A. Kitazawa and K. Okamoto: Phys. Rev. B 62 (2000) 940; K. Okamoto and A. Kitazawa: J. Phys. Chem. Solids 62 (2001) 365.
- 4) A. Kitazawa: J. Phys. A: Math. Gen. 30 (1997) L285.
- 5) K. Nomura and A. Kitazawa: J. Phys. A: Math. Gen. 31 (1998) 7341.
- 6) S. R. White: Phys. Rev. Lett. 69 (1992) 2863; Rev. B 48 (1993) 10345.
- 7) Z. L. Berezinskii: Zh. Eksp. Teor. Fiz. 61 (1971) 1144 (Sov. Phys.-JETP 34 (1971) 610); J. M. Kosterlitz and D. J. Thouless, J. Phys. C: Solid State Phys. 6 (1973) 1181.
- 8) The algorithm used in the computer program package KOBEPACK has been discussed by M. Kaburagi, T. Tonegawa and T. Nishino [Computational Approaches in Condensed Matter Physics, Springer Proc. Phys., ed. S. Miyashita, M. Imada and H. Takayama (Springer, Berlin, 1992) p. 179].
- 9) J. C. Bonner and M. E. Fisher: Phys. Rev. 135 (1964) A 640.
- 10) The case of $J = 1$ has already been studied by T. Tonegawa: Prog. Theor. Phys., Suppl., No. 46 (1970) 61.